Draft version April 10, 2013
Preprint typeset using LaTeX style emulateapj v. 5/2/11

arXiv:1304.2392v1 [astro-ph.SR] 8 Apr 2013

# *MOST* OBSERVATIONS OF $\sigma$ ORI E: CHALLENGING THE CENTRIFUGAL BREAKOUT NARRATIVE

R. H. D. Townsend[1], Th. Rivinius[2], J. F. Rowe[3], A. F. J. Moffat[4], J. M. Matthews[5], D. Bohlender[6], C. Neiner[7], J. H. Telting[8], D. B. Guenther[9], T. Kallinger[10,5], R. Kuschnig[10,5], S. M. Rucinski[11], D. Sasselov[12], W. W. Weiss[10]

*Draft version April 10, 2013*

## ABSTRACT

We present results from three weeks' photometric monitoring of the magnetic helium-strong star $\sigma$ Ori E using the *MOST* microsatellite. The star's light curve is dominated by twice-per-rotation eclipse-like dimmings arising when magnetospheric clouds transit across and occult the stellar disk. However, no evidence is found for any abrupt centrifugal breakout of plasma from the magnetosphere, either in the residual flux or in the depths of the light minima. Motivated by this finding we compare the observationally inferred magnetospheric mass against that predicted by a breakout analysis. The large discrepancy between the values leads us to argue that centrifugal breakout does not play a significant role in establishing the magnetospheric mass budget of $\sigma$ Ori E.

*Subject headings:* stars: individual (HD 37479) — stars: magnetic fields — stars: rotation — stars: chemically peculiar — stars: early-type — circumstellar matter

## 1. INTRODUCTION

The B2Vpe star $\sigma$ Ori E (HD 37479) is a magnetic helium-strong star characterized by variations in many of its observables, including photometric indices (Hesser et al. 1977), H$\alpha$ emission (Walborn 1974; Bolton 1974; Reiners et al. 2000), photospheric and wind absorption lines (Pedersen & Thomsen 1977; Groote & Hunger 1982; Shore & Brown 1990), radio emission (Leone & Umana 1993), linear continuum polarization (Kemp & Herman 1977; Carciofi et al. 2013) and circular line polarization (Landstreet & Borra 1978; Oksala et al. 2012). The variability originates from surface abundance inhomogeneities, together with plasma trapped in a circumstellar magnetosphere with the highest densities in co-rotating cloud-like structures situated at the intersections between magnetic and rotational equators (e.g. Groote & Hunger 1982; Bolton et al. 1987; Shore 1993; Townsend et al. 2005). Townsend et al. (2010) recently discovered that the 1.19 d rotation period is gradually lengthening due to magnetic braking.

Building on previous work by Nakajima (1985), Townsend & Owocki (2005) developed a *rigidly-rotating magnetosphere* (RRM) model to explain the shape of the star's magnetosphere. Radiatively driven wind streams flowing up from the photosphere are channeled into head-on collisions by closed magnetic loops. After shock heating and subsequent radiative cooling the near-stationary plasma settles into magnetohydrostatic equilibrium, supported against the inward pull of gravity by the centrifugal force arising from enforced co-rotation. The predicted plasma distribution appears to be in good agreement with observations (Townsend et al. 2005, hereafter T05), although there are some discrepancies (e.g., Carciofi et al. 2013) which warrant further investigation.

For such a wind-fed magnetosphere, the total mass of trapped plasma necessarily must grow with time unless a countervailing mass leakage mechanism allows some kind of balance to be reached. Townsend & Owocki (2005) proposed a mechanism involving the stressing and eventual breaking of magnetic loops by the centrifugal force, which grows in strength as plasma accumulates. Magnetohydrodynamic (MHD) simulations by ud-Doula et al. (2006) support this *centrifugal breakout* hypothesis, and moreover suggest that the reconnection heating arising during breakout episodes could explain the X-ray flares seen in $\sigma$ Ori E (over and above its quiescent wind-shock emission) by Groote & Schmitt (2004) and Sanz-Forcada et al. (2004). However, no direct evidence of breakout has so far been found.

In this paper we present data from three weeks' photometric monitoring of $\sigma$ Ori E by the *MOST* microsatellite (Walker et al. 2003), beginning November 2007. The motivation for this observing campaign was to better characterize the star's light curve, and to search for any cycle-to-cycle changes arising from putative centrifugal breakout episodes. Section 2 describes the observations and

townsend@astro.wisc.edu
[1] Department of Astronomy, University of Wisconsin-Madison, 2535 Sterling Hall, 475 N. Charter Street, Madison, WI 53706, USA
[2] ESO - European Organisation for Astronomical Research in the Southern Hemisphere, Casilla 19001, Santiago 19, Chile
[3] NASA Ames Research Center, Moffett Field, CA 94035, USA
[4] Départment de physique, Université de Montréal C.P. 6128, Succursale Centre-Ville, Montréal, QC H3C 3J7, Canada
[5] Department of Physics and Astronomy, University of British Columbia, 6224 Agricultural Road, Vancouver, BC V6T 1Z1, Canada
[6] National Research Council of Canada, Herzberg Institue of Astrophysics, 5071 West Saanich Road, Victoria, BC, V9E 2E7, Canada
[7] LESIA, UMR 8109 du CNRS, Observatoire de Paris, UPMC, Université Paris Diderot, 5 place Jules Janssen, 92195, Meudon Cedex, France
[8] Nordic Optical Telescope, Apartado 474, 38700 Santa Cruze de La Palma, Spain
[9] Department of Astronomy and Physics, St. Marys University, Halifax, NS B3H 3C3, Canada
[10] University of Vienna, Institute for Astronomy, Türkenschanzstrasse 17, A-1180 Vienna, Austria
[11] Dept. of Astronomy and Astrophysics, University of Toronto, 50 St George Street, Toronto, ON M5S 3H4, Canada
[12] Harvard-Smithsonian Center for Astrophysics, 60 Garden Street, Cambridge, MA 02138, USA

explains the procedure used to reduce the raw data, and Section 3 analyzes various aspects of the light curve. The findings are discussed in Section 4 and then summarized in Section 5.

## 2. OBSERVATIONS AND DATA REDUCTION

*MOST* observed $\sigma$ Ori E and four other nearby bright B-type stars (HD 37525; $\sigma$ Ori D; HD 37744; HD 294272) over the interval November 12 – December 3 2007 with a cadence of around 60 s. The satellite operated in direct imaging mode, where targets are placed on the open area of the science CCD not covered by the Fabry microlens array (see Rowe et al. 2006b,a); this comes at the cost of a degraded instrumental stability and precision, but is necessary because $\sigma$ Ori E is too faint ($V = 6.66$) to observe in Fabry mode. Individual subexposures of 0.530 s were co-added onboard the satellite prior to downloading, to avoid saturating the telemetry link (see Rowe et al. 2008). The number of subexposures per co-added exposure was initially set at 31, but was then increased to 61 after the first 17 hours of the run.

At the beginning of the run $\sigma$ Ori E fell outside the *MOST* continuous viewing zone (CVZ); therefore, for $\sim$ 25 minutes of every 101.413-minute orbit the satellite slewed to observe an alternative field in the Hyades, resulting in periodic gaps in the data (see the top two rows of Fig. 1). On November 23 the star entered the CVZ and *MOST* switched to observing it continuously. Around half a day prior to this switch the onboard computer crashed, leading to a $\sim 0.25$ d gap in the data. The orientation of the spacecraft after the switch initially led to increased solar heating and a climb in the CCD temperature, accounting for certain features in the residual light curve discussed below. Finally, gaps in the data on December 2 and December 3 arose due to science data buffer overruns.

The co-added exposures of $\sigma$ Ori E, each a 20 by 20 pixel image, are reduced using the standard approach of synthetic aperture photometry. The stellar flux is calculated as the difference between the total flux in a 5-pixel radius circular aperture centered on the 2-dimensional Gaussian centroid of the image, and the estimated background flux. A complication peculiar to *MOST*'s direct imaging mode is that the background flux includes stray light contributions which are spatially inhomogeneous and modulate with the satellite's orbit (Reegen et al. 2006). To remove these artifacts we follow the procedure described by Rowe et al. (2006b,a) with some modifications. The correlation between the pre-whitened stellar flux and the background flux is fit using locally weighted regression (Cleveland 1979), with a tri-cubed weight function and a smoothing parameter $f = 0.084$ chosen by 10-fold cross validation (Arlot & Celisse 2010). The pre-whitening subtracts a periodic signal representing the intrinsic variability of $\sigma$ Ori E, which would otherwise distort the flux correlation fit. To determine this signal we apply locally weighted regression to the phase-folded stellar flux, with a smoothing parameter $f = 0.019$ again determined by cross validation and a period $P = 1.190847$ d chosen by minimizing the weighted mean square error of the regression. The 68.2% confidence interval of this period determination is $\Delta P = \pm 0.000015$ d (determined via bootstrap Monte-Carlo simulations; e.g., Press et al. 1992), and so the period is in good agreement with the $P = 1.198051 \pm 0.000003$ d predicted by the Townsend et al. (2010) ephemeris.

Fig. 1 plots the light curve resulting from this reduction process, together with the periodic signal determined for the pre-whitening. These data clearly reveal the signature twice-per-rotation eclipse-like dimmings of the star arising when the magnetospheric clouds transit across and occult the stellar disk. Allowing for the different photometric responses, no gross differences stand out between the *MOST* light curve and historical observations (e.g., Hesser et al. 1977; Pedersen & Thomsen 1977; Groote & Hunger 1982).

## 3. ANALYSIS

Figure 2 shows the residual flux after pre-whitening the light curve with the periodic signal. A $\pm 0.1$ d boxcar mean curve, together with the associated one-standard-deviation bounds, is plotted below the points to highlight long-term trends in the data. This smoothed curve clearly reveals an abrupt dimming by about 0.0035 mag near the mid-point of the observations ($t - 2454416.5 \approx 11$ d), together with a reduction in the standard deviation. Also visible in the curve is a low-level ripple with a frequency $\sim 1 - 2\,\mathrm{d}^{-1}$. However, the corresponding smoothed light curve of HD 37744 (also shown in the figure) reveals similar behavior in both respects; hence, neither the dimming nor the ripple can be intrinsic to $\sigma$ Ori E. The effects are likely instrumental in origin; the dimming in particular is correlated with a sharp 5 K increase in the temperature of the CCD pre-amplifier, due to the increased solar heating which occurred when *MOST* switched to continuous observation of $\sigma$ Ori E (see Sec. 2).

Apart from these instrumental variations, the smoothed curve in Fig. 2 is relatively devoid of features. In particular, there are no obvious flares characterized by a sudden brightening of the star followed by a slow decline. One interpretation of this result is that there were no centrifugal breakout episodes during the *MOST* run, since any breakout would be accompanied by a large release of magnetic energy. A caveat, however, is that although a link between magnetic reconnection and optical flaring has been established in other types of systems (e.g., weak-line T Tauri stars — Fernández et al. 2004; M dwarfs — Stelzer et al. 2006), the same cannot be said for the centrifugally supported magnetospheres considered here. The MHD breakout simulations by ud-Doula et al. (2006) cannot offer much guidance, since they are unable to predict how much emission will be produced at optical wavelengths.

In addition to flaring, centrifugal breakout episodes might reveal themselves through abrupt and ongoing reductions in the magnetospheric column density. To search for these signatures we measure the depths of the primary and secondary minima in the light curve, across the 20 rotation cycles spanned by the observing run. While the depths show cycle-to-cycle changes at a level $\sim 0.002$ mag which exceeds the formal error bars, these variations occur in both directions and appear more consistent with the instrumental variations mentioned in the previous section than with any evolution in the column density.

## 4. DISCUSSION

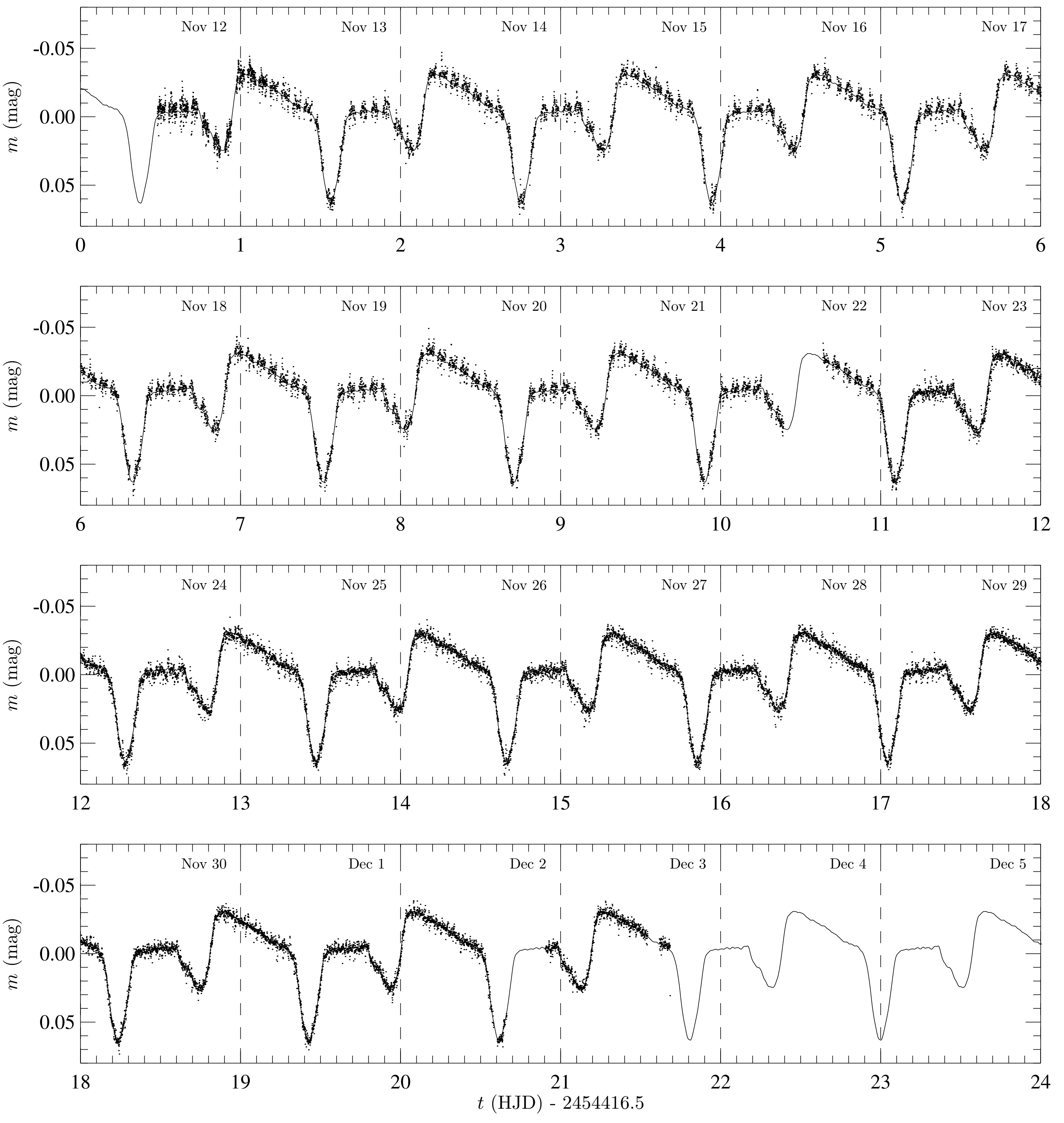


FIG. 1.— The stellar flux $m$ of $\sigma$ Ori E, in magnitudes relative to the mean flux, plotted as a function of time. The solid curve overlaying the data shows the periodic signal used for pre-whitening. The vertical dashed lines delineate the day boundaries.

| $M_*(\mathrm{M}_\odot)$ | $R_*(\mathrm{R}_\odot)$ | $\Omega$ ( $\Omega_c$) | $B_*$ (kG) | $\beta$ (°) | $\epsilon_*$ |
|---|---|---|---|---|---|
| 8.30 | 3.77 | 0.454 | 11.0 | 55 | $10^{-3}$ |

TABLE 1
PARAMETERS ADOPTED IN CALCULATING THE INFERRED MAGNETOSPHERE MASS $M_{\mathrm{mag}}$ AND ASYMPTOTIC MAGNETOSPHERE MASS $M_\infty$ OF $\sigma$ ORI E.

The failure to find any evidence for centrifugal breakout episodes, either in the form of optical flares in the residual flux or as systematic changes in the depths of the light minima, could be due simply to unlucky scheduling of the *MOST* run coupled with the fact that the breakout recurrence timescale is poorly constrained (as it depends on the unknown wind mass-loss rate). However, there are a number of independent arguments which favor the alternative conclusion that centrifugal breakout simply *does not occur* in $\sigma$ Ori E, at least at a level where it has any impact on the magnetospheric mass budget.

Foremost amongst these is the discrepancy between the magnetospheric mass $M_{\mathrm{mag}}$ inferred from analysis of the

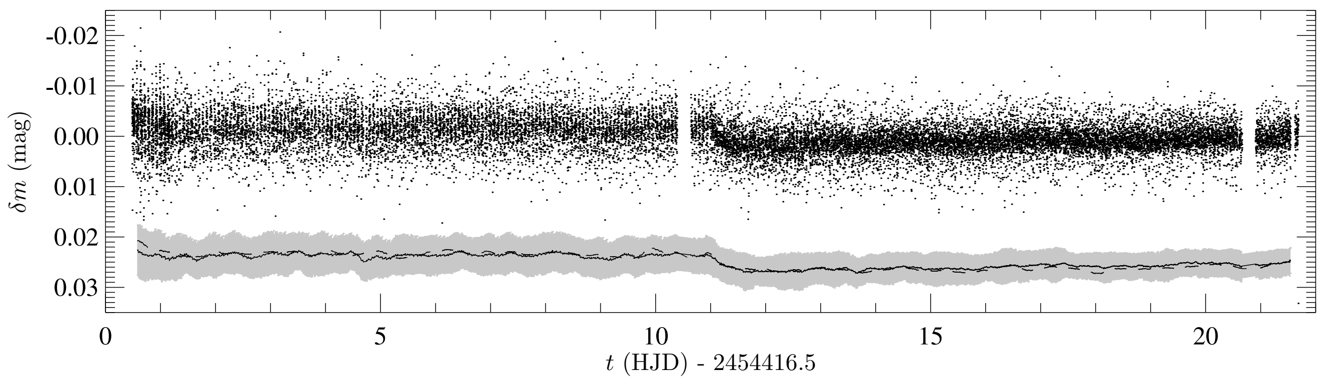


FIG. 2.— The residual stellar flux $\delta m$, in magnitudes relative to the mean flux, plotted as a function of time. The solid curve beneath (shifted down by 0.025 mag for clarity) shows the $\pm 0.1$ d boxcar mean curve, with the gray envelope illustrating the associated one-standard-deviation bounds. For comparison, the dashed curve shows the corresponding smoothed light curve of HD 37744.

observations using the RRM model, and the asymptotic magnetosphere mass $M_\infty$ predicted by the breakout analysis of Townsend & Owocki (2005, their Appendix A2); if centrifugal breakout plays a role in governing the magnetospheric mass budget then these two values should be comparable. Table 1 lists the stellar and magnetosphere parameters adopted here to evaluate $M_{\rm mag}$ and $M_\infty$; the field strength $B_*$, magnetic obliquity $\beta$ and magnetosphere scale-height parameter $\epsilon_*$ are taken from T05, while the other parameters are derived in Appendix A. Applying the light-curve synthesis procedure described by T05, the RRM model requires $\rho_{\rm max}\kappa R_* \approx 7$ to reproduce the observed depth $\approx 0.065$ mag of the primarily light minima, with $\rho_{\rm max}$ being the maximum mass density in the magnetosphere, $\kappa$ the flux-mean opacity in the *MOST* passband, and $R_*$ the stellar radius. A lower limit on the opacity is given by the electron scattering value, $\kappa_{\rm es} = 0.34\,{\rm cm^2\,g^{-1}}$ for a fully ionized solar-abundance composition. With $R_* = 3.77\,{\rm R_\odot}$ from Table 1, we therefore obtain an upper limit $\rho_{\rm max} \lesssim 8 \times 10^{-11}\,{\rm g\,cm^{-3}}$ on the maximum density. Integrating over the RRM density distribution leads to a corresponding upper mass limit $M_{\rm mag} \lesssim 2 \times 10^{-10}\,{\rm M_\odot}$. This is almost two orders of magnitude smaller than the asymptotic mass $M_\infty = 1.2 \times 10^{-8}\,{\rm M_\odot}$ predicted by the breakout analysis, indicating that the magnetosphere is well short of the level required for *significant* breakout episodes to occur.

With hindsight, this result didn't have to wait for the *MOST* observations presented here. Certainly, these observations provide an unprecedentedly precise characterization of the (remarkably unchanging) light curve of $\sigma$ Ori E, which provokes our re-examination of centrifugal breakout. However, the same general conclusions will be reached if a similar analysis is applied to the original Hesser et al. (1977) light curve (or for that matter any other photometric observations of the star), since the depths of the minima in these historic data are similar to those in Fig. 1. We also note that the spectroscopic measurements by Groote & Hunger (1982) independently indicate $M_{\rm mag} \approx 10^{-10}\,{\rm M_\odot}$, and the recent linear polarization measurements by Carciofi et al. (2013) likewise give $M_{\rm mag} \approx 2 \times 10^{-11}\,{\rm M_\odot}$ — both consistent with the upper limit derived above. Presumably the larger figure derived by Groote & Hunger (1982) results from their assumption of a vertical magnetosphere extent $\sim 1\,R_*$, rather larger than the $\sim 0.2\,R_*$ predicted by the RRM model.

Further corroborating arguments against breakout are presented in a forthcoming paper (Townsend et al., in preparation), which demonstrates that the low-mass companion discovered by Bouy et al. (2009) is responsible for the majority of the X-ray flux from the $\sigma$ Ori E system. It seems likely that the X-ray flares proposed to arise during breakout (Sec. 1) instead come from the magnetic activity of the companion, as originally conjectured by Sanz-Forcada et al. (2004).

These findings challenge a prevailing narrative for mass leakage from centrifugally supported magnetospheres. It is natural to now ask what other leakage mechanism(s) might be at work to balance the continual feeding of plasma from the wind, as evidenced by the star's rotationally modulated UV absorption lines (Shore & Brown 1990). Havnes & Goertz (1984) explore cross-field diffusive processes such as ambipolar diffusion, but find them far too slow to be effective; revisiting their calculations with updated stellar parameters does not change this conclusion. A related question concerns the process(es) responsible for magnetospheric features not predicted by the RRM model — for instance, the substructure seen in the secondary light minima in Fig. 1, and the departures from the expected mass distribution revealed in the linear polarization measurements by Carciofi et al. (2013). Corresponding departures can also be seen in photometric and spectroscopic observations of a number of other He-strong stars harboring magnetospheres (e.g., HR 7355 — Oksala et al. 2010; Rivinius et al. 2010, 2012; $\delta$ Ori C — Leone et al. 2010; HR 5907 — Grunhut et al. 2012). Are these a consequence of the as-yet-unidentified mass-leakage mechanism, or instead due to a non-dipole field topology? In the case of $\sigma$ Ori E, recent spectropolarimetric measurements by Oksala et al. (2012) indeed reveal deviations from dipolarity, although these are not consistent with the decentered dipole invoked by T05 to explain the overall difference in the depths of the primary and secondary light minima. Clearly, there remains much work to be done in understanding the effects of mass redistribution, mass leakage and field topology in governing the distribution and overall amount of plasma in these stars' magnetospheres.

Looking toward the future, a logical next step is to decompose the *MOST* light curve into magnetospheric

and photospheric components, the latter arising from the inhomogeneous abundance distribution across the stellar surface. Krtička et al. (2007, 2011) have successfully used surface abundance maps derived from Doppler imaging to reproduce the photospheric light variations of other He-strong stars. A similar approach should be possible for $\sigma$ Ori E, once the process of deriving the abundance maps is complete (see Oksala et al. 2012). The decomposed light curve will allow quantitative testing of the hypothesis (e.g., T05) that the brightening seen after the secondary minima is photospheric rather than magnetospheric in origin. Likewise, comparing the magnetospheric component against the light-curve morphologies predicted by the RRM model (see Townsend 2008) will allow further refinement of the model and moreover offer insights into the as-yet-unknown mechanisms responsible for mass leakage.

## 5. SUMMARY

We have presented new photometric observations of $\sigma$ Ori E obtained using the *MOST* microsatellite (Sec. 2). Despite the unprecedented precision of the light curve no evidence is found for centrifugal breakout episodes or any other variability beyond rotational modulation, either in the residual flux or in the depths of the light minima (Sec. 3). Motivated by this finding we compare the observationally inferred magnetospheric mass against the asymptotic mass predicted by the Townsend & Owocki (2005) breakout analysis (Sec. 4). The former is around two orders of magnitude smaller than the latter, leading us to rule out centrifugal breakout as a mechanism for significant magnetospheric mass leakage in $\sigma$ Ori E.

RHDT acknowledges support from NSF awards AST-0908688 and AST-0904607, and NASA award NNX12AC72G. AFJM, DBG, JMM and SMR are grateful for financial support from NSERC (Canada). RK and WW acknowledge support by the Austrian Science Fund, P22691-N16.

## APPENDIX

### FUNDAMENTAL PARAMETERS OF $\sigma$ ORI E

Groote & Hunger (1982) determine an effective temperature $T_{\rm eff} = 22\,500\,{\rm K}$ for $\sigma$ Ori E by fitting the spectral energy distribution from UV through to IR. They likewise derive a surface gravity $\log g = 3.85\,{\rm dex}$ from modeling H and He equivalent widths. A subsequent more-detailed analysis of Balmer-line wings led Hunger et al. (1989) to revise this value slightly upwards, to $\log g = 3.95\,{\rm dex}$. As discussed by these latter authors, the $T_{\rm eff}$ and $\log g$ together imply that $\sigma$ Ori E is more distant ($\sim 650\,{\rm pc}$) than the $\sigma$ Ori cluster ($\sim 450\,{\rm pc}$), and is moreover a factor $\sim 10$ older than the cluster. These findings, however, stand contrary to a number of observational results indicating that $\sigma$ Ori E is a bona fide member of the cluster rather than a background star. The reddening of $\sigma$ Ori E is the same as $\sigma$ Ori AB (Sherry et al. 2008), and likewise for the interstellar polarization (Kemp & Herman 1977; Carciofi et al. 2013). The radial velocity and proper motion of $\sigma$ Ori E are indistinguishable from those of the cluster (Caballero 2007). Finally, the spindown measurements by Townsend et al. (2010) indicate that the star is young, with an age $\sim 1.1\,{\rm Myr}$ consistent with lower-end age estimates for the cluster.

The problem with the Hunger et al. (1989) analysis likely resides in the surface gravity determination. Emission from magnetospheric plasma fills in the wings of Balmer lines; if not properly corrected this makes the lines appear less broad, and the gravity consequently smaller, than is actually the case. Given this complication it seems better to avoid the gravity measurement altogether, and derive stellar parameters using a different approach. Accordingly, assuming $\sigma$ Ori E is a cluster member, a radius $R_* = 3.77\,{\rm R}_\odot$ follows from the angular diameter $\theta = 0.079\,{\rm mas}$ (Groote & Hunger 1982) and the cluster distance $d = 444\,{\rm pc}$ derived for solar metallicity by Sherry et al. (2008).

To obtain the corresponding mass, we calculate a sequence of solar-metallicity evolutionary tracks with masses $M_* = 7, 7.1, 7.2, \ldots, 9.9, 10\,{\rm M}_\odot$ using the MESA stellar evolution code (Paxton et al. 2011). For simplicity the calculations neglect the effects of rotation. The $M_* = 8.3\,{\rm M}_\odot$ track passes closest to $T_{\rm eff} = 22\,500\,{\rm K}$, $R_* = 3.77\,{\rm R}_\odot$ point, and we adopt this as the stellar mass. With the measured rotation period (Sec. 2) the dimensionless angular velocity is $\omega = \Omega/\Omega_{\rm c} = 0.454$, where $\Omega_{\rm c} = \sqrt{8GM_*/27R_*^3}$ is the critical angular velocity.

## REFERENCES

Arlot, S., & Celisse, A. 2010, Statistics Surveys, 4, 40
Bolton, C. T. 1974, ApJ, 192, L7
Bolton, C. T., Fullerton, A. W., Bohlender, D., Landstreet, J. D., & Gies, D. R. 1987, in IAU Colloq. 92: Physics of Be Stars, ed. A. Slettebak & T. P. Snow, 82
Bouy, H., Huélamo, N., Martín, E. L., et al. 2009, A&A, 493, 931
Caballero, J. A. 2007, A&A, 466, 917
Carciofi, A. C., Faes, D. M., Townsend, R. H. D., & Bjorkman, J. E. 2013, ApJ, 766, L9
Cleveland, W. S. 1979, J. American Statistical Association, 74, 829
Fernández, M., Stelzer, B., Henden, A., et al. 2004, A&A, 427, 263
Groote, D., & Hunger, K. 1982, A&A, 116, 64
Groote, D., & Schmitt, J. H. M. M. 2004, A&A, 418, 235
Grunhut, J. H., Rivinius, T., Wade, G. A., et al. 2012, MNRAS, 419, 1610
Havnes, O., & Goertz, C. K. 1984, A&A, 138, 421
Hesser, J. E., Ugarte, P. P., & Moreno, H. 1977, ApJ, 216, L31
Hunger, K., Heber, U., & Groote, D. 1989, A&A, 224, 57
Kemp, J. C., & Herman, L. C. 1977, ApJ, 218, 770
Krtička, J., Marková, H., Mikulášek, Z., et al. 2011, in IAU Symposium, Vol. 272, Active OB Stars: Mass-Loss, Rotation and Critical Limits, ed. C. Neiner, G. Wade, G. Meynet, & G. Peters, 517
Krtička, J., Mikulášek, Z., Zverko, J., & Žižňovský, J. 2007, A&A, 470, 1089
Landstreet, J. D., & Borra, E. F. 1978, ApJ, 224, L5
Leone, F., Bohlender, D. A., Bolton, C. T., et al. 2010, MNRAS, 401, 2739
Leone, F., & Umana, G. 1993, A&A, 268, 667
Nakajima, R. 1985, Ap&SS, 116, 285
Oksala, M. E., Wade, G. A., Marcolino, W. L. F., et al. 2010, MNRAS, 405, L51

Oksala, M. E., Wade, G. A., Townsend, R. H. D., et al. 2012, MNRAS, 419, 959
Paxton, B., Bildsten, L., Dotter, A., et al. 2011, ApJS, 192, 3
Pedersen, H., & Thomsen, B. 1977, A&AS, 30, 11
Press, W. H., Teukolsky, S. A., Vetterling, W. T., & Flannery, B. P. 1992, Numerical recipes in FORTRAN, 2nd edn. (Cambridge University Press, Cambridge UK)
Reegen, P., Kallinger, T., Frast, D., et al. 2006, MNRAS, 367, 1417
Reiners, A., Stahl, O., Wolf, B., Kaufer, A., & Rivinius, T. 2000, A&A, 363, 585
Rivinius, T., Szeifert, T., Barrera, L., et al. 2010, MNRAS, 405, L46
Rivinius, T., Townsend, R. H. D., Kochukhov, O., et al. 2012, MNRAS, submitted
Rowe, J. F., Matthews, J. M., Seager, S., et al. 2006a, ApJ, 646, 1241
Rowe, J. F., Matthews, J. M., Kuschnig, R., et al. 2006b, Mem. Soc. Astron. Italiana, 77, 282
Rowe, J. F., Matthews, J. M., Seager, S., et al. 2008, ApJ, 689, 1345
Sanz-Forcada, J., Franciosini, E., & Pallavicini, R. 2004, A&A, 421, 715
Sherry, W. H., Walter, F. M., Wolk, S. J., & Adams, N. R. 2008, AJ, 135, 1616
Shore, S. N. 1993, in Astronomical Society of the Pacific Conference Series, Vol. 44, IAU Colloq. 138: Peculiar versus Normal Phenomena in A-type and Related Stars, ed. M. M. Dworetsky, F. Castelli, & R. Faraggiana, 528
Shore, S. N., & Brown, D. N. 1990, ApJ, 365, 665
Smith, M. A., & Bohlender, D. A. 2007, A&A, 475, 1027
Stelzer, B., Schmitt, J. H. M. M., Micela, G., & Liefke, C. 2006, A&A, 460, L35
Townsend, R. H. D. 2008, MNRAS, 389, 559
Townsend, R. H. D., Oksala, M. E., Cohen, D. H., Owocki, S. P., & ud-Doula, A. 2010, ApJ, 714, L318, (T10)
Townsend, R. H. D., & Owocki, S. P. 2005, MNRAS, 357, 251
Townsend, R. H. D., Owocki, S. P., & Groote, D. 2005, ApJ, 630, L81, (T05)
ud-Doula, A., Townsend, R. H. D., & Owocki, S. P. 2006, ApJ, 640, L191
Walborn, N. R. 1974, ApJ, 191, L95
Walker, G., Matthews, J., Kuschnig, R., et al. 2003, PASP, 115, 1023